Atmos. Chem. Phys. Discuss., doi:10.5194/acp-2015-871, 2016
Manuscript under review for journal Atmos. Chem. Phys.
Published: 15 January 2016

Atmospheric Chemistry and Physics Discussions

Impact of molecular structure on secondary organic aerosol formation from aromatic hydrocarbon photooxidation under low NO_x conditions

L. Li[1,2], P. Tang[1,2], S. Nakao[1,2,a], and D. R. Cocker III[1,2]

[1]University of California, Riverside, Department of Chemical and Environmental Engineering, Riverside, CA 92507, USA
[2]College of Engineering-Center for Environmental Research and Technology (CE-CERT), Riverside, CA 92507, USA
[a]currently at: Clarkson University, Department of Chemical and Biomolecular Engineering, Potsdam, NY 13699, USA

Received: 24 October 2015 – Accepted: 26 November 2015 – Published: 15 January 2016

Correspondence to: D. R. Cocker III (dcocker@engr.ucr.edu)

Published by Copernicus Publications on behalf of the European Geosciences Union.

Abstract

The molecular structure of volatile organic compounds (VOC) determines their oxidation pathway, directly impacting secondary organic aerosol (SOA) formation. This study comprehensively investigates the impact of molecular structure on SOA formation from the photooxidation of twelve different eight to nine carbon aromatic hydrocarbons under low NO_x conditions. The effects of the alkyl substitute number, location, carbon chain length and branching structure on the photooxidation of aromatic hydrocarbons are demonstrated by analyzing SOA yield, chemical composition and physical properties. Aromatic hydrocarbons, categorized into five groups, show a yield order of ortho (*o*-xylene and *o*-ethyltoluene) > one substitute (ethylbenzene, propylbenzene and isopropylbenzene) > meta (*m*-xylene and *m*-ethyltoluene) > three substitute (trimethylbenzenes) > para (*p*-xylene and *p*-ethyltoluene). SOA yields of aromatic hydrocarbon photooxidation do not monotonically decrease when increasing alkyl substitute number. The ortho position promotes SOA formation while the para position suppresses aromatic oxidation and SOA formation. Observed SOA chemical composition and volatility confirm that higher yield is associated with further oxidation. SOA chemical composition also suggests that aromatic oxidation increases with increasing alkyl substitute chain length and branching structure. Further, carbon dilution theory developed by Li et al. (2015a) is extended in this study to serve as a standard method to determine the extent of oxidation of an alkyl substituted aromatic hydrocarbon.

1 Introduction

Organic aerosols are critical to human health (Dockery et al., 1993; Krewski et al., 2003; Davidson et al., 2005), climate change (IPPC, 2007) and visibility (Pöschl, 2005; Seinfeld and Pandis, 2006). Global anthropogenic secondary organic aerosol (SOA) sources are underestimated by current models (Henze et al., 2008; Matsui et al., 2009; Hallquist et al., 2009; Farina et al., 2010) and have larger growth potential than biogenic

ACPD
doi:10.5194/acp-2015-871

aerosol sources due to the increase of known anthropogenic emissions (Heald et al., 2008). Therefore, it is crucial to explore SOA formation mechanism from anthropogenic precursors.

Aromatic hydrocarbons are major anthropogenic SOA precursors (Kanakidou et al., 2005; Henze et al., 2008; Derwent et al., 2010). C_8 (ethylbenzene, xylenes) and C_9 (ethyltoluenes and trimethylbenzenes) aromatics are important aromatic hydrocarbons in the atmosphere besides toluene and benzene (Monod et al., 2001; Millet et al., 2005; Heald et al., 2008; Kansal et al., 2009; Hu et al., 2015). The major sources of C_8 and C_9 aromatic hydrocarbons are fuel evaporation (Kaiser et al., 1992; Rubin et al., 2006; Miracolo et al., 2012), tailpipe exhaust (Singh et al., 1985; Monod et al., 2001; Lough et al., 2005; Na et al., 2005; Correa and Arbilla et al., 2006) and solvent use (Zhang et al., 2013). C_8 aromatic hydrocarbons (ethylbenzene and xylenes (ortho, meta and para) are categorized as hazardous air pollutants (HAPs) under the US Clean Air Act Amendments of 1990 (http://www.epa.gov/ttnatw01/orig189.html). Toluene and C_8 aromatics dominate anthropogenic SOA and SOA yield from all C_9 aromatics is currently predicted to be equal to that of toluene (Bahreini et al., 2009). The chemical composition of aromatic SOA remains poorly understood with less than 50 % of aromatic hydrocarbon photooxidation products identified (Forstner et al., 1997; Fisseha et al., 2004; Hamilton et al., 2005; Sato et al., 2007). Aromatic hydrocarbon photooxidation mechanisms remain uncertain except for the initial step ($\sim$ 90 % OH-addition reaction) (Calvert et al., 2002). Hence, understanding the atmospheric reaction mechanisms of C_8 and C_9 aromatic hydrocarbons and properly quantifying their SOA formation potential present unique challenges due to the variety in their molecular structure and the electron density of the aromatic ring.

Volatile organic compound (VOC) structure impacts the gas phase reaction mechanism (Ziemman and Atkinson, 2012) and kinetic reaction rate (e.g. k_{OH} Atkinson, 1987) thereby influencing the resulting SOA properties and mass yield. Molecular structure impacts on SOA formation from alkanes have been previously studied (Lim and Ziemann, 2009; Ziemann, 2011; Lambe et al., 2012; Tkacik et al., 2012; Yee et al., 2013;

ACPD
doi:10.5194/acp-2015-871

Loza et al., 2014). It is generally observed that SOA yield decreases from cyclic alkanes to linear alkanes and to branched alkanes. The relative location of the methyl group on the carbon chain also affects SOA yield (Tkacik et al., 2012). It is further found that the SOA yield and structure relationship is influenced by C=C groups (Ziemann, 2011). Understanding the SOA yield and structure relationship of aromatic compounds in a similar way is necessary due to the atmospheric importance of aromatic hydrocarbons.

Previously, aromatic studies categorized SOA yield solely based on substitute number (Odum, 1997a, b). However, those chamber experiments were conducted at high NO_x conditions, which are well above levels present in the atmosphere. Song et al. (2005, 2007) found that initial HC/NO_x ratios significantly impact SOA yields during aromatic photooxidation with yields increasing as NO_x levels decreased. Ng et al. (2007) shows there is no significant yield difference between one substitute (toluene) and two substitute (*m*-xylene) aromatics in the absence of NO_x. The current work focuses on molecular structure impact on SOA formation at more atmospherically relevant NO_x and aerosol loadings. Li et al. (2015a) demonstrated the methyl group number impact on SOA formation under low NO_x conditions. Also, aromatic compounds with para position alkyl groups have been observed to form less SOA under various NO_x conditions than their isomers in previous studies. Izumi and Fukuyama (1990) found that *p*-xylene, *p*-ethyltoluene and 1,2,4-trimethylbenzene have low SOA formation potential under high NO_x conditions. Song et al. (2007) observed that *p*-xylene has the smallest SOA yield among all xylenes in the presence of NO_x. The relative methyl position to -OH in dimethyl phenols also impacts SOA yield in the absence of NO_x (Nakao et al., 2011), while Song et al. (2007) observed no significant SOA yield difference between *o*-xylene and *p*-xylene under NO_x free conditions. Moreover, previous studies mainly focused on the carbon number effect on SOA formation (Lim and Ziemann, 2009; Li et al., 2005a) and seldom addressed the substitute carbon length impact on VOC oxidation and hence SOA formation. Different percentages of similar compounds are found when the substitute carbon length on the aromatic ring changes

ACPD
doi:10.5194/acp-2015-871

(Forstner et al., 1997; Huang et al., 2007, 2011). For example, a higher percentage of 3-methyl-2,5-furanone is observed in toluene than that of 3-ethyl-2,5-furanone in ethylbenzene (Forstner et al., 1997). Further, the branching structure on the aromatic substitute might impact the reaction pathway. It is possible that fragmentation is more favored on branched substitute alkoxy radicals than *n*-alkane substituents similar to alkanes (Atkinson et al., 2003).

Few studies comprehensively consider the overall alkyl effect on SOA formation from aromatic hydrocarbons, including the substitute number, position, carbon chain length and branching structure, especially under low NO_x conditions. It is valuable to understand the relationship between aromatic hydrocarbon molecular structures and SOA physical and chemical characteristics. The effects of OH exposure (Lambe et al., 2011, 2015), mass loading (Shilling et al., 2009; Pfaffenberger et al., 2013) and NO condition (Ng et al., 2007; Eddingsaas et al., 2012) on SOA physical and chemical characteristics are previously discussed. However, few studies address the molecular structure effect of the precursor on SOA chemical composition, especially under atmospherically relevant conditions. Sato et al. (2012) shows the chemical composition difference between ethylbenzene, *m*-xylene, *o*-xylene, 1,2,4-trimethylbenzene and 1,3,5-trimethylbenzene under high absolute NO_x conditions and hypothesizes that ketones prevent further oxidation during aromatic photooxidation compared with aldehydes. The SOA products detected in Sato's study are mainly small volatile compounds which are less likely to partition into the particle phase (Chhabra et al., 2011). Therefore, the study of Sato et al. (2012) indicates that further oxidation or oligmerization might contribute to SOA formation during aromatic photooxidation. Less SOA characterization data on propylbenzene and ethyltoluene compared with trimethylbenzene is available. However, Bahreini et al. (2009) suggests that the sum of the propylbenzene and ethyltoluene is on average a factor of 4–10 more abundant than trimethylbenzene.

This work examines twelve aromatic hydrocarbons, all of which are isomers with eight or nine carbons, to investigate the impact of molecular structure on SOA formation from aromatic hydrocarbon photooxidation under low NO_x. Here, we investigate the

ACPD
doi:10.5194/acp-2015-871

substitute number, substitute position, alkyl carbon chain length and alkyl branching impacts on aromatic hydrocarbon oxidation.

2 Method

2.1 Environmental chamber

The UC Riverside/CE-CERT indoor dual 90 m^3 environmental chambers were used in this study and are described in detail elsewhere (Carter et al., 2005). Experiments were all conducted at dry conditions (RH < 0.1 %), in the absence of inorganic seed aerosol and with temperature controlled to 27 ± 1 °C. Two movable top frames were slowly lowered during each experiment to maintain a slight positive differential pressure (~ 0.02″ H_2O) between the reactors and enclosure to minimize dilution and/or contamination of the reactors. 272 115 W Sylvania 350BL blacklights are used as light sources for photooxidation.

A known volume of high purity liquid hydrocarbon precursors (ethylbenzene Sigma-Aldrich, 99.8 %; *n*-propylbenzene Sigma-Aldrich, 99.8 %; isopropylbenzene Sigma-Aldrich, analytical standard; *m*-xylene Sigma-Aldrich, 99 %; *o*-xylene Sigma-Aldrich, 99 %; *p*-xylene Sigma-Aldrich, 99 %; *m*-ethyltoluene Sigma-Aldrich, 99 %; *o*-ethyltoluene Sigma-Aldrich, 99 %; *p*-ethyltoluene Sigma-Aldrich, ≥ 95 %; 1,2,3-trimethylbenzene Sigma-Aldrich, OEKANAL analytical standard; 1,2,4-trimethylbenzene Sigma-Aldrich, 98 %; 1,3,5-trimethylbenzene Sigma-Aldrich, analytical standard) was injected through a heated glass injection manifold system and flushed into the chamber with pure N_2. NO was introduced by flushing pure N_2 through a calibrated glass bulb filled to a predetermined partial pressure of pure NO. All hydrocarbons and NO are injected and well mixed before lights are turned on to start the experiment.

ACPD
doi:10.5194/acp-2015-871

2.2 Particle and gas measurement

Particle size distribution between 27 and 686 nm was monitored by dual custom built Scanning Mobility Particle Sizers (SMPS) (Cocker et al., 2001). Particle effective density was measured with an Aerosol Particle Mass Analyzer (APM-SMPS) system (Malloy et al., 2009). Particle volatility was measured by a Dekati® Thermodenuder Volatility Tandem Differential Mobility Analyzer (VTDMA) (Rader and McMurry, 1986) with a 17 s heating zone residence time (Qi et al., 2010a). The heating zone was controlled to 100 °C in this study with Volume fraction remaining (VFR) calculated as $(D_{\text{p, after TD}}/D_{\text{p, before TD}})^3$.

Particle-phase chemical composition evolution was measured by a High Resolution Time of Flight Aerosol Mass Spectrometer (HR-ToF-AMS; Aerodyne Research Inc.) (Canagaratna et al., 2007; DeCarlo et al., 2006). The sample was vaporized by a 600 °C oven followed by a 70 eV electron impact ionization. f_x in this study is calculated as the fraction of the organic signal at $m/z = x$. For example, f_{44}, f_{43}, f_{57} and f_{71} are the ratios of the organic signal at m/z 44, 43, 57 and 71 to the total organic signal, respectively (Chhabra et al., 2011; Duplissy et al., 2011). Elemental ratios for total organic mass, oxygen to carbon (O/C), and hydrogen to carbon (H/C) were determined using the elemental analysis (EA) technique (Aiken et al., 2007, 2008). Data was analyzed with ToF-AMS analysis toolkit squirrel 1.56D/PIKA 1.15D version.

The Agilent 6890 Gas Chromatograph – Flame Ionization Detector was used to measure aromatic hydrocarbon concentrations. A Thermal Environmental Instruments Model 42C chemiluminescence NO analyzer was used to monitor NO, NO_y-NO and NO_y. The gas-phase reaction model SAPRC-11 developed by Carter and Heo (2012) was utilized to predict radical concentrations (·OH, HO_2·, RO_2· and NO_3·).

ACPD
doi:10.5194/acp-2015-871

3 Result

3.1 SOA yield

Photooxidation of twelve C_8 and C_9 aromatic hydrocarbons were studied for low NO_x conditions (HC/NO ratio 11.1–171 ppbC:ppb). SOA yields for all aromatic hydrocarbons were calculated according to Odum et al. (1996) as the mass ratio of aerosol formed to parent hydrocarbon reacted. Experimental conditions and SOA yields are listed (Table 1) along with additional *m*-xylene, *o*-xylene, *p*-xylene and 1,2,4-trimethylbenzene experimental conditions from previous studies (Song et al., 2005; Li et al., 2015a) (Table S2 in the Supplement). SOA yield as a function of particle mass concentration (M_0), shown in Fig. 1, includes experiments listed in both Tables 1 and S2. Each symbol represents a different aromatic hydrocarbon. It is observed that both alkyl substitute number and position affect SOA yield. The SOA yield of two-substitute C_8 and C_9 aromatic hydrocarbons depends more on the substitute location than substitute length. This means that the yield trend of *o*-xylene is analogous to that of *o*-ethyltoluene. Similarly, the yield trends for meta and para position substituted C_8 and C_9 aromatic hydrocarbons will be analogous to each other. Ortho isomers (*o*-xylene and *o*-ethyltoluene, marked as solid and hollow green circles, respectively) have the highest SOA yield for similar aerosol concentrations while para isomers (*p*-xylene and *p*-ethyltoluene, marked as solid and hallow blue diamonds, respectively) have the lowest SOA yield level. Lower SOA yield for para isomers are consistent with previous observation by Izumi and Fukuyama (1990). Izumi and Fukuyama (1990) also suggest that 1,2,4-trimethylbenzene yields are lower than for other aromatic hydrocarbons. The current study does not show a significant SOA yield difference between 1,2,4-trimethylbenzene and 1,3,5-trimethylbenzene. It is difficult to compare 1,2,3-trimethylbenzene yields with the former two trimethylbenzenes since 1,2,3-trimethylbenzene mass loading is much higher than the former two.

Aromatic hydrocarbons having only one substitute (ethylbenzene, *n*-propylbenzene and isopropylbenzene) or three substitutes (1,2,3-trimethylbenzene, 1,2,4-

ACPD
doi:10.5194/acp-2015-871

trimethylbenzene and 1,3,5-trimethylbenzene) tend to have yields similar to the meta position two alkyl aromatics. Odum et al. (1997b) categorized SOA yield formation potential solely based on substitute number and claimed that aromatics with less than two methyl or ethyl substitutes form more particulate matter than those with two or more methyl or ethyl substitutes on the aromatic ring. However, Odum's work was conducted for high NO_x conditions and had insufficient data to compare isomer yield differences (e.g., only two low mass loadings for *o*-xylene data). The strong low yield (two or more substitutes) and high yield (less than two methyl or ethyl substitutes) trends for high NO_x conditions (Odum et al., 1997) are not observed for low NO_x aromatic experiments in this study. Rather, high yield is observed only for benzene (Li et al., 2015a) while low yield is seen for substituted aromatic hydrocarbons. Similar SOA yield trends from different C_8 and C_9 aromatic isomers are further confirmed by comparing yields at similar radical conditions (Table S4, Fig. S2 in the Supplement). It is also found that molecular structure exerts a greater impact on SOA yield than reaction kinetics (Supplement). A two product model described by Odum et al. (1996) is used to fit SOA yield curves as a function of M_0. The twelve aromatics are categorized into five groups to demonstrate the alkyl group number and position effect on SOA formation. The five groups include one substitute group (1S), ortho position two alkyl group (ortho), meta position two alkyl group (meta), para position two alkyl group (para) and three substitute group (3S). Fitting parameters (α_1, $K_{om,1}$, α_2 and $K_{om,2}$; Table 2) in the two product model are determined by minimizing the sum of the squared residuals. The lower volatility partitioning parameter ($K_{om,2}$) is the same for all yield curve fits by assuming similar high volatile compounds are formed during all aromatic hydrocarbon photooxidation experiments. The ortho group is associated with a much higher $K_{om,1}$ compared with other aromatic groups, indicating aromatic hydrocarbon oxidation with an ortho position substitute forms much lower volatility products than other isomers. $K_{om,1}$ are also slightly higher in the meta group and one substitute groups than in the three substitute and para substitute groups.

ACPD
doi:10.5194/acp-2015-871

A slight SOA yield difference remains within each group (Fig. S1 and Table S3 in the Supplement), indicating the influence of factors other than alkyl group position. Generally, lower yields are found in aromatics with higher carbon number substitute alkyl groups, such as when comparing propylbenzene (*i*- and *n*-) with ethylbenzene or toluene (Li et al., 2005a), *m*-ethyltoluene with *m*-xylene and *p*-ethyltoluene with *p*-xylene, respectively. These differences are explained by the proposed alkyl group dilution effect (Sect. 4).

3.2 Chemical composition

3.2.1 f_{44} vs. $f_{43+57+71}$

The ratio of alkyl substitute carbon number (H : C > 1) to the aromatic ring carbon number impacts SOA composition since the H : C ratio on the alkyl substitute is larger than 1 and the H : C ratio on aromatic ring itself is no more than 1. m/z 43 ($C_2H_3O^+$ and $C_3H_7^+$) combined with m/z 44 (CO_2^+) are critical to characterize oxygenated compounds in organic aerosol (Ng et al., 2010, 2011). $C_2H_3O^+$ is the major contributor to m/z 43 in SOA formed from aromatic hydrocarbons having only methyl substitute (Li et al., 2015a) while $C_3H_7^+$ fragments are observed in this work for SOA from propylbenzene and isopropylbenzene (Fig. S4 in the Supplement). The $C_nH_{2n-1}O^+$ fragment in SOA corresponds to a C_nH_{2n+1}-alkyl substitute to the aromatic ring. $C_3H_5O^+$ (m/z 57) and $C_4H_7O^+$ (m/z 71) are important when investigating SOA from ethyl or propyl substitute aromatic precursors. While m/z 43 ($C_3H_7^+$) and 57 ($C_4H_9^+$) are often considered as markers for hydrogen-like organic aerosol (Zhang et al., 2015; Ng et al., 2010), $C_3H_5O^+$ (m/z 57) and $C_4H_7O^+$ (m/z 71) are the major fragments (Fig. S4) from SOA originating from ethyl and propyl substituted aromatics, consistent with Sato et al. (2010) and Mohr et al. (2009). Figure S4 lists all fragments found at m/z 43, 44, 57 and 71 and Fig. S5 in the Supplement shows the fraction of each m/z in SOA formed from all aromatic hydrocarbons studied. The m/z 43 + m/z 44 + m/z 57 + m/z 71 accounts for 21.2 to 29.5 % of the total mass fragments from all C_8 and C_9 aromatics studied, suggesting

ACPD
doi:10.5194/acp-2015-871

similar oxidation pathways. Only a small fraction (<~ 0.7 %) of m/z 71 ($C_4H_7O^+$) or m/z 57 ($C_3H_5O^+$) was observed in ethyltoluenes and trimethylbenzenes, respectively.

Figure S3 in the Supplement shows the evolution of f_{44} and $f_{43+57+71}$ in SOA formed from the photooxidation of different aromatic hydrocarbons at low NO_x conditions. f_{44} and $f_{43+57+71}$ ranges are comparable to previous chamber studies (Ng et al., 2010; Chhabra et al., 2011; Loza et al., 2012; Sato et al., 2012). Only slight f_{44} and $f_{43+57+71}$ evolution during chamber photooxidation is observed for the C_8 and C_9 isomers hence only the average f_{44} and $f_{43+57+71}$ will be analyzed in this work.

A modification is applied to the mass based m/z fraction in order to compare the mole relationship between m/z 44 and m/z 43 + m/z 57 + m/z 71 (Eq. 1).

$$f'_{43+57+71} = \frac{44}{43} f_{43} + \frac{44}{57} f_{57} + \frac{44}{71} f_{71} \quad (1)$$

The average f_{44} vs. $f'_{43+57+71}$ for all C_8 and C_9 isomers (Fig. 2) are located around the trend line for methyl group substituted aromatic hydrocarbons (Li et al., 2015a), implying a similarity in the SOA components formed from alkyl substituted aromatic hydrocarbons. A decreasing trend in oxidation from upper left to lower right is included in Fig. 2, similar to what Ng et al. (2011) found in the f_{44} vs. f_{43} graph, especially while comparing similar structure compounds. The methyl group location on the aromatic ring impacts f_{44}: $f'_{43+57+71}$. Decreasing f_{44} and increasing $f'_{43+57+71}$ trends are observed from *p*-xylene to *o*-xylene to *m*-xylene and from 1,2,4-trimethylbenzene to 1,2,3-trimethylbenzene to 1,3,5-trimethylbenezene. The $f'_{43+57+71}$ may partially depend on the relative position between the alkyl substitute and the peroxide oxygen of the bicyclic hydroperoxide. For instance, allylically stabilized five-membered bicyclic radicals are the most stable bicyclic peroxide formed from aromatic hydrocarbon photooxidation (Andino et al., 1996). Two meta position substitutes connected to the aromatic ring carbon with -C-O- yield higher fractions of $C_nH_{2n-1}O^+$ fragments than the para and ortho position, which have at most one substitute connected with -C-O-. More importantly, the difference in f_{44} implies that substitute location influences the further reaction

ACPD
doi:10.5194/acp-2015-871

pathway to form CO_2^+ since CO_2^+ is not readily available from bicyclic hydroperoxides. This indicates that the alkyl groups are more likely to contribute to SOA formation at the meta position than the ortho and para position. The para position substituted aromatics form the least SOA as they exclude the possibility that para position alkyl substitutes are further oxidized to other less volatile components instead of $C_nH_{2n-1}O^+$. *p*-Xylene displays the high f_{44} similar to benzene (Li et al., 2015a) implying that the para position substitute exerts the least dilution effect on CO_2^+ formation pathway among all isomers. Bicyclic hydroperoxides formed from the OH-addition reaction pathway and their dissociation reaction products are both used to explain the substitute location impact on f_{44} and $f'_{43+57+71}$ relationship. However, the existence of longer alkyl substitutes diminishes the alkyl substitute location impact. SOA f_{44} and $f'_{43+57+71}$ in ethyltoluenes are all analogous to *m*-xylene. One substitute C_8 and C_9 aromatic hydrocarbons have similar f_{44} and $f'_{43+57+71}$ with slightly lower f_{44} and $f'_{43+57+71}$ compared to toluene (Li et al., 2015a). Longer alkyl substitutes may not lower the average oxidation per mass as further oxidation of the longer chain alkyls may render other oxidized components not included in Fig. 2. Their lower total f_{44}+ $f'_{43+57+71}$ (Fig. S5) further supports the possibility of oxidation of the longer alkyl substitutes. Elemental ratio (Sect. 3.2.2) and oxidation state (Sect. 3.2.3) are further used to evaluate the impact of increasing alkyl group size on SOA formation.

3.2.2 H/C vs. O/C

Elemental analysis (Aiken et al., 2007, 2008) serves as a valuable tool to elucidate SOA chemical composition and SOA formation mechanisms (Heald et al., 2010; Chhabra et al., 2011). Figure S6 in the Supplement shows H/C and O/C evolution in SOA formed from the photooxidation of different aromatic hydrocarbons under low NO_x (marked and colored similarly to Fig. S3). H/C and O/C ranges are comparable to previous chamber studies (Chhabra et al., 2011 (*m*-xylene and toluene); Loza et al., 2012 (*m*-xylene); Sato et al., 2012 (benzene and 1,3,5-trimethylbenzene)). SOA components from all isomers are located in between slope = −1 and slope = −2 lines (Fig. S6) sug-

ACPD
doi:10.5194/acp-2015-871

gesting that SOA from these aromatic hydrocarbons is composed primarily of acid (carbonyl acid and hydroxycarbonyl) and carbonyl (ketone or aldehyde) like functional groups. The elemental ratio of SOA from *p*-xylene photooxidation was nearly located on the acid line (slope = −1). The SOA elemental ratio for C_8 and C_9 aromatic isomers are located near the alkyl number trend line found by Li et al. (2015a) for methyl substituents, indicating a similarity between SOA from various alkyl substituted hydrocarbons. SOA formed is among the LV-OOA and SV-OOA regions (Ng et al., 2011). The evolution trend agrees with Fig. S3 (Sect. 3.2.1). The current study concentrated on experimentally averaged H/C and O/C to explore the impact of molecular structure on SOA chemical composition.

Average H/C and O/C locations are marked with aromatic compound names in Fig. 3. All H/C and O/C are located around the predicted values for C_8 and C_9 SOA (dark solid circle) based on the elemental ratio of benzene SOA (Li et al., 2015a). This confirms the presence of a carbon dilution effect in all isomers. Ortho position aromatic hydrocarbons (*o*-xylene or *o*-ethyltoluene) lead to a more oxidized SOA (higher O/C and lower H/C) than that of meta (*m*-xylene or *m*-ethyltoluene) and para (*p*-xylene or *p*-ethyltoluene) aromatics. SOA formed from 1,2,4-trimethylbenzene and 1,2,3-trimethylbenzene is more oxidized than that from 1,3,5-trimethylbenzene. It is noticed that 1,2,4-trimethylbenzene and 1,2,3-trimethylbenzene both contain an ortho position moiety on the aromatic ring. This indicates that the ortho position aromatic hydrocarbon is readily oxidized and this ortho position impact on oxidation extends to triple substituted aromatic hydrocarbons.

Substitute length also plays an important role in aromatic hydrocarbon oxidation. Overall, SOA from a one-substitute aromatic with more carbon in the substitute is located at a more oxidized area of the O/C vs. H/C chart (lower right in Fig. 3.) than those multiple substitute aromatic isomers with the same total number of carbon as the single substituted aromatic. SOA from isopropylbenzene is located in a lower position of the chart and to the right of propylbenzene indicating that branch carbon structure on the alkyl substitute of aromatic hydrocarbons leads to a more oxidized SOA. Lines

ACPD
doi:10.5194/acp-2015-871

in Fig. S7 in the Supplement connect the O/C and H/C of resulting SOA to that of the aromatic precursor. Most SOA components show a slight H/C increase and a dramatic O/C increase from the precursor, which is consistent with results observed for methyl substituted aromatics (Li et al., 2015a). However, H/C barely increases (1.33 to 1.34) from the propylbenzene precursor to its resulting SOA and there is even a decreasing trend from isopropylbenzene to its SOA. This indicates that a high H/C component loss reaction such as alkyl part dissociation during photooxidation is an important reaction to SOA formation from longer carbon chain containing aromatic hydrocarbons. The carbon chain length of propylbenzene increases the possibility of alkyl fragmentation. The branching structure of isopropylbenzene facilitates fragmentation through the stability of tertiary alkyl radicals. Elemental ratio differences between xylenes and ethyltoluenes can be attributed to the alkyl dilution effect, similar to the methyl dilution theory by Li et al. (2015a). *m*-Ethyltoluene is an exception as it is more oxidized than *m*-xylene after accounting for the alkyl dilution effect. This suggests that the meta substituted longer chain alkyl is more readily oxidized since the substitute is at the end of ring opening products. Prediction of elemental ratios from toluene and xylenes are discussed later (Sect. 4) to further quantify the carbon length and branching effect on SOA formation from aromatic hydrocarbons.

3.2.3 OS_c

Oxidation state ($OS_c \approx 2O/C\text{-}H/C$) was introduced into aerosol phase component analysis by Kroll et al. (2011). It is considered to be a more accurate metric for describing oxidation in atmospheric organic aerosol (Ng et al., 2009; Canagaratna et al., 2015; Lambe et al., 2015) and therefore well correlated with gas-particle partitioning (Aumont et al., 2012;). Average OS_c of SOA formed from C_8 and C_9 aromatic isomers ranges from −0.53 to −0.20 and −0.82 to −0.22, respectively (Fig. 4), implying that the precursor molecular structure impacts the OS_c of the resulting SOA. An OS_c decrease with alkyl substitute length is observed in one-substitute aromatic hydrocarbons from toluene (toluene OS_c = −0.049; Li et al., 2015a) to propylben-

ACPD
doi:10.5194/acp-2015-871

zene. However, OS_c provides the average oxidation value per carbon not considering whether these carbons start from an aromatic ring carbon or an alkyl carbon. Alkyl carbons are associated with more hydrogen than aromatic ring carbons, thus leading to a lower precursor OS_c and therefore lower SOA OS_c. Dilution theory in Sect. 4 will be used to further explore the carbon chain length effect on aromatic hydrocarbon oxidation by considering the precursor H : C ratio. Single substitute aromatic hydrocarbons generally show higher OS_c than multiple substitute ones, consistent with the yield trend of Odum et al. (1997b). However, it is also found that ortho position moiety containing two or three substitute aromatic hydrocarbons have analogous OS_c to single substitute aromatic hydrocarbons (*o*-xylene −0.202 to ethylbenzene −0.197; 1,2,4-trimethylbenzene −0.433 and *o*-ethyltoluene −0.492 to propylbenzene −0.435). This suggests that both substitute number and position are critical to aromatic hydrocarbon oxidation and therefore SOA formation. OS_c trends also support that the meta position suppresses oxidation while the ortho position promotes oxidation when the OS_c of xylenes (*o*-xylene > *p*-xylene > *m*-xylene), ethyltoluenes (*o*-ethyltoluene > *p*-ethyltoluene > *m*-ethyltoluene) and trimethylbenzenes (1,2,4-trimethylbenzene (ortho moiety containing) > 1,2,3-trimethylbenzene (ortho moiety containing) > 1,3,5-trimethylbenzene (meta moiety containing)) are compared separately. Further, SOA formed from isopropylbenzene shows the highest OS_c among all C_9 isomers, nearly equivalent to that of ethylbenzene. This demonstrates that the branching structure of the alkyl substitute can enhance further oxidation of aromatic hydrocarbons.

3.3 Physical property

3.3.1 SOA density

SOA density is a fundamental parameter in understanding aerosol morphology, dynamics, phase and oxidation (De Carol et al., 2004; Katrib et al., 2005; Dinar et al., 2006; Cross et al., 2007). SOA density ranges from 1.29–1.38 g cm^{-3} from aromatic photooxidation under low NO_x conditions in this study (Fig. 5). The range is comparable to

ACPD
doi:10.5194/acp-2015-871

previous studies under similar conditions (Esther Borrás and Tortajada-Genaro, 2012; Ng et al., 2007; Sato et al., 2010). There is no significant difference in the density of SOA formed from C_8 and C_9 aromatic hydrocarbon isomers and molecular structure is not observed to be a critical parameter to determine SOA density. The standard deviation results from differences in initial conditions (e.g., initial HC/NO) that also determine the oxidation of aromatic hydrocarbons (Li et al., 2015b) and thus further affect density. SOA density is best correlated with the O/C ratio and OS_c (0.551 and 0.540, Table 3), consistent with the observation of Pang et al. (2006) that SOA density increases with increasing O/C ratio. The density prediction method developed by Kuwata et al. (2011) based on O/C and H/C is evaluated as

$$\rho = \frac{12 + \mathrm{H/C} + 16 \times \mathrm{O/C}}{7 + 5 \times \mathrm{H/C} + 4.15 \times \mathrm{O/C}} \quad (2)$$

The black lines (Fig. 5) are predicted (Eq. 2) densities and show a good agreement between predicted and measured SOA densities (−6.01 to 6.90 %).

3.3.2 SOA volatility

SOA volatility is associated with reactions such as oxidation, fragmentation, oligomerization and mass loading (Kalberer et al., 2004; Salo et al., 2011; Tritscher et al., 2011; Yu et al., 2014). SOA volatility in this study is measured as VFR. Initial (< 30 min after new particle formation) SOA VFRs are around 0.2 for all the aromatic precursors studied and increase up to 0.58 during photooxidation. This suggests that aromatic hydrocarbon oxidation undergoes an evolution from volatile compounds to semivolatile compounds. The VFR trends and ranges are comparable to previous studies (Kalberer et al., 2004; Qi et al., 2010a, b; Nakao et al., 2012). Figure 6 shows the VFR at the end of aromatic hydrocarbon photooxidation (VFR_{end}). A decreasing VFR_{end} trend is found as the number of substitutes increase and for meta position (e.g. *m*-xylene) or meta position containing (e.g. 1,3,5-trimethylbenzene) aromatic precursors. Strong correlations

ACPD
doi:10.5194/acp-2015-871

among VFR_{end} and chemical composition are observed in the aromatic hydrocarbons studied here (Table 3). This is consistent with recent findings that O : C ratio is well correlated to aerosol volatility (Sect. 3.3.2) (Cappa et al., 2012; Yu et al., 2014), thereby affecting the gas-particle partitioning, which in turn relates to SOA yield. It is also observed that VFR_{end} is strongly correlated (−0.937) with reaction rate constant (k_{OH}). Higher k_{OH} is associated with faster reaction rates of initial aromatic precursors and is therefore expected to lead to further oxidation for a given reaction time. However, the inverse correlation between k_{OH} and VFR_{end} indicates that k_{OH} value represents more than just the kinetic aspects. k_{OH} increases with increasing number of substitutes on the aromatic ring. Additionally, aromatic hydrocarbons with meta position substitutes have higher k_{OH} than those with para and ortha (Table S1 in the Supplement) position substitutes. This suggests that the precursor molecular structures for aromatics associated with k_{OH} values determine the extent of oxidation of the hydrocarbons and therefore impact SOA volatility more than simply the precursor oxidation rate.

4 Alkyl dilution theory on SOA formation from aromatic hydrocarbons

The dependence of SOA formation on molecular structure can be partially represented by the alkyl carbon number. Methyl dilution theory (Li et al., 2015a) is extended to alkyl substitute dilution theory in order to investigate the influence of longer alkyl substitutes compared with methyl group substitutes. Figure 7a shows the predicted elemental ratio for SOA formed from longer alkyl substitutes ($-C_2H_{2n+1}$, $n > 1$) based on methyl only substitute. The elemental ratio of SOA formed from single substitute aromatic hydrocarbons including ethylbenzene, propylbenzene and isopropylbenzene are predicted by toluene and those of ethyltoluenes are predicted by corresponding xylenes with similar alkyl substitute location. H/C and O/C are generally overestimated by only considering alkyl dilution effect. However, OS_c prediction is close to measurement (> ±15 %; Fig. 7b and dashed line in Fig. 7a) for ethyltoluenes. This suggests that higher carbon number alkyl substitutes may suppress reactions that have little effect on OS_c but large effect

ACPD
doi:10.5194/acp-2015-871

on elemental ratio (e.g hydrolysis). OS_c is largely underestimated in SOA formed from single substitute aromatic hydrocarbons, especially for isopropylbenzene and ethylbenzene. This implies that longer alkyl substitutes are more oxidized than the methyl group on toluene. A direct •OH reaction with the alkyl part of the aromatic is more favored on longer alkyl chains since tertiary and secondary alkyl radicals are more stable than primary alkyl radicals (Forstner et al., 1997). The less significant OS_c underestimation from xylenes to ethyltoluenes is due to the presence of an "inert" methyl group which lowers the average OS_c. The extreme low H/C in isopropylbenzene implies an additional hydrogen loss with the branching alkyl substitute, which possibly occurs while forming 2,5-furandione (Forstner et al., 1997) or 3-H-furan-2-one due to the increased stability of the isopropyl radical compared to the *n*-propyl radical. It is also possible that longer carbon chain substitutes might have higher probability to form other cyclic or low vapor pressure products by additional reaction due to their increased length. The similarity in f_{44} and $f'_{43+57+71}$ but discrepancy in elemental ratio among all single substitute C_8 and C_9 aromatics supports that additional reactions leading to further oxidization of alkyl substitutes can occur.

5 Atmospheric implication

This study elucidates molecular structure impact on a major anthropogenic SOA source, photooxidation of aromatic hydrocarbons, under atmospherically relevant NO_x conditions by analyzing SOA yield, chemical composition and physical properties. These observations, when taken together, indicate the roles of alkyl substitute number, location, carbon chain length and branching structure in aromatic hydrocarbon photooxidation. SOA yield of all C_8 and C_9 aromatic hydrocarbon isomers are comprehensively provided in this study with a focus on the impact of molecular structure. It is demonstrated that aromatic hydrocarbon oxidation and SOA formation should not be simply explained by substitute number. The promoting of SOA formation by the ortho position is found along with confirmation of the suppression effect by the para

ACPD
doi:10.5194/acp-2015-871

position during oxidation of aromatic hydrocarbons. Meta position alkyl substitutes on aromatic ring lead to a lower extend of aromatic hydrocarbon oxidation. Aromatic oxidation is proved to increase with alkyl substitute chain length and branching structure. Further, carbon dilution theory developed by Li et al. (2015a) is extended to this study. Carbon dilution theory not only serves as a tool to explain the difference in SOA components due to the difference in substitute alkyl carbon number but also acts as a standard to determine the oxidation mechanism based on alkyl substitute structure. This study improves the understanding of SOA formation from aromatic hydrocarbons and contributes to more accurate SOA prediction from aromatic precursors. Further study is warranted to reveal the detailed oxidation pathway of aromatic hydrocarbons with longer (carbon number > 1) alkyl substitutes.

Acknowledgements. We acknowledge funding support from National Science Foundation (ATM 0901282) and W. M. Keck Foundation. Any opinions, findings, and conclusions expressed in this material are those of the author(s) and do not necessarily reflect the views of the NSF.

References

Aiken, A. C., DeCarlo, P. F., and Jimenez, J. L.: Elemental analysis of organic species with electron ionization high-resolution mass spectrometry, Anal. Chem., 79, 8350–8358, doi:10.1021/ac071150w, 2007.

Aiken, A. C., DeCarlo, P. F., Kroll, J. H., Worsnop, D. R., Huffman, J. A., Docherty, K. S., Ulbrich, I. M., Mohr, C., Kimmel, J. R., Sueper, D., Sun, Y., Zhang, Q., Trimborn, A., Northway, M., Ziemann, P. J., Canagaratna, M. R., Onasch, T. B., Alfarra, M. R., Prevot, A. S. H., Dommen, J., Duplissy, J., Metzger, A., Baltensperger, U., and Jimenez, J. H.: O/C and OM/OC ratios of primary, secondary, and ambient organic aerosols with high-resolution time-of-flight aerosol mass spectrometry, Environ. Sci. Technol., 42, 4478–4485, doi:10.1021/es703009q, 2008.

Andino, J. M., Smith, J. N., Flagan, R. C., Goddard, W. A., and Seinfeld, J. H.: Mechanism of atmospheric photooxidation of aromatics: a theoretical study, J. Phys. Chem.-US, 100, 10967–10980, doi:10.1021/jp952935l, 1996.

ACPD

doi:10.5194/acp-2015-871

Atkinson, R.: A structure–activity relationship for the estimation of rate constants for the gas-phase reactions of OH radicals with organic compounds, Int. J. Chem. Kinet., 19, 799–828, doi:10.1002/kin.550190903, 1987.

Atkinson, R. and Arey, J.: Atmospheric degradation of volatile organic compounds, Chem. Rev., 103, 4605–4638, doi:10.1021/cr0206420, 2003.

Aumont, B., Valorso, R., Mouchel-Vallon, C., Camredon, M., Lee-Taylor, J., and Madronich, S.: Modeling SOA formation from the oxidation of intermediate volatility *n*-alkanes, Atmos. Chem. Phys., 12, 7577–7589, doi:10.5194/acp-12-7577-2012, 2012.

Bahreini, R., Ervens, B., Middlebrook, A., Warneke, C., De Gouw, J., DeCarlo, P., Jimenez, J., Brock, C., Neuman, J., Ryerson, T., Stark, H., Atlas, E., Brioude, J., Fried, A., Holloway, J. S., Peischl, J., Richter, D., Walega, J., Weibring, P., Wollny, A. G., and Fehsenfeld, F. C.: Organic aerosol formation in urban and industrial plumes near Houston and Dallas, Texas, J. Geophys. Res.-Atmos., 114, D00F16, doi:10.1029/2008JD011493, 2009.

Borrás, E. and Tortajada-Genaro, L. A.: Secondary organic aerosol formation from the photo-oxidation of benzene, Atmos. Environ., 47, 154–163, doi:10.1016/j.atmosenv.2011.11.020, 2012.

Calvert, J. G., Atkinson, R., Becker, K. H., Kamens, R. M., Seinfeld, J. H., Wallington, T. J., and Yarwood, G.: The Mechanisms of Atmospheric Oxidation of Aromatic Hydrocarbons, Oxford University Press, New York, 2002.

Canagaratna, M. R., Jayne, J. T., Jimenez, J. L., Allan, J. D., Alfarra, M. R., Zhang, Q., Onasch, T. B., Drewnick, F., Coe, H., Middlebrook, A., Delia, A., Williams, L. R., Trimborn, A. M., Northway, M. J., DeCarlo, P. F., Kolb, C. E., Davidovits, P., and Worsnop, D. R.: Chemical and microphysical characterization of ambient aerosols with the aerodyne aerosol mass spectrometer, Mass. Spectrom. Rev., 26, 185–222, doi:10.1002/mas.20115, 2007.

Canagaratna, M. R., Jimenez, J. L., Kroll, J. H., Chen, Q., Kessler, S. H., Massoli, P., Hildebrandt Ruiz, L., Fortner, E., Williams, L. R., Wilson, K. R., Surratt, J. D., Donahue, N. M., Jayne, J. T., and Worsnop, D. R.: Elemental ratio measurements of organic compounds using aerosol mass spectrometry: characterization, improved calibration, and implications, Atmos. Chem. Phys., 15, 253–272, doi:10.5194/acp-15-253-2015, 2015.

Cappa, C. D. and Wilson, K. R.: Multi-generation gas-phase oxidation, equilibrium partitioning, and the formation and evolution of secondary organic aerosol, Atmos. Chem. Phys., 12, 9505–9528, doi:10.5194/acp-12-9505-2012, 2012.

ACPD

doi:10.5194/acp-2015-871

Carter, W. P. L., Cocker III, D. R., Fitz, D. R., Malkina, I. L., Bumiller, K., Sauer, C. G., Pisano, J. T., Bufalino, C., and Song, C.: A new environmental chamber for evaluation of gas-phase chemical mechanisms and secondary aerosol formation, Atmos. Environ., 39, 7768–7788, doi:10.1016/j.atmosenv.2005.08.040, 2005.

Carter, W. P. L. and Heo, G.: Development of Revised SAPRC Aromatics Mechanisms, Report to the California Air Resources Board Contracts (07-730), 2012.

Chhabra, P. S., Ng, N. L., Canagaratna, M. R., Corrigan, A. L., Russell, L. M., Worsnop, D. R., Flagan, R. C., and Seinfeld, J. H.: Elemental composition and oxidation of chamber organic aerosol, Atmos. Chem. Phys., 11, 8827–8845, doi:10.5194/acp-11-8827-2011, 2011.

Cocker III, D. R., Flagan, R. C., and Seinfeld, J. H.: State-of-the-art chamber facility for studying atmospheric aerosol chemistry, Environ. Sci. Technol., 35, 2594–2601, doi:10.1021/es0019169, 2001.

Correa, S. M. and Arbilla, G.: Aromatic hydrocarbons emissions in diesel and biodiesel exhaust, Atmos. Environ., 40, 6821–6826, doi:10.1016/j.atmosenv.2006.05.068, 2006.

Cross, E. S., Slowik, J. G., Davidovits, P., Allan, J. D., Worsnop, D. R., Jayne, J. T., Lewis, D. K., Canagaratna, M., and Onasch, T. B.: Laboratory and ambient particle density determinations using light scattering in conjunction with aerosol mass spectrometry, Aerosol Sci. Tech., 41, 343–359, doi:10.1080/02786820701199736, 2007.

Davidson, C. I., Phalen, R. F., and Solomon, P. A.: Airborne particulate matter and human health: a review, Aerosol Sci. Tech., 39, 737–749, doi:10.1080/02786820500191348, 2005.

DeCarlo, P. F., Kimmel, J. R., Trimborn, A., Northway, M. J., Jayne, J. T., Aiken, A. C., Gonin, M., Fuhrer, K., Horvath, T., Docherty, K. S., Worsnop, D. R., and Jimenez, J. L.: Field-deployable, high-resolution, time-of-flight aerosol mass spectrometer, Anal. Chem., 78, 8281–8289, doi:10.1021/ac061249n, 2006.

DeCarlo, P. F., Slowik, J. G., Worsnop, D. R., Davidovits, P., and Jimenez, J. L.: Particle morphology and density characterization by combined mobility and aerodynamic diameter measurements, Part 1: Theory, Aerosol Sci. Tech., 38, 1185–1205, doi:10.1080/027868290903907, 2004.

Derwent, R. G., Jenkin, M. E., Utembe, S. R., Shallcross, D. E., Murrells, T. P., and Passant, N. R.: Secondary organic aerosol formation from a large number of reactive man-made organic compounds, Sci. Total. Environ., 408, 3374–3381, doi:10.1016/j.scitotenv.2010.04.013, 2010.

ACPD

doi:10.5194/acp-2015-871

Dinar, E., Mentel, T. F., and Rudich, Y.: The density of humic acids and humic like substances (HULIS) from fresh and aged wood burning and pollution aerosol particles, Atmos. Chem. Phys., 6, 5213–5224, doi:10.5194/acp-6-5213-2006, 2006.

Dockery, D. W., Pope, C. A., Xu, X., Spengler, J. D., Ware, J. H., Fay, M. E., Ferris Jr., B. G., and Speizer, F. E.: An association between air pollution and mortality in six US cities, New. Engl. J. Med., 329, 1753–1759, doi:10.1056/NEJM199312093292401, 1993.

Duplissy, J., DeCarlo, P. F., Dommen, J., Alfarra, M. R., Metzger, A., Barmpadimos, I., Prevot, A. S. H., Weingartner, E., Tritscher, T., Gysel, M., Aiken, A. C., Jimenez, J. L., Canagaratna, M. R., Worsnop, D. R., Collins, D. R., Tomlinson, J., and Baltensperger, U.: Relating hygroscopicity and composition of organic aerosol particulate matter, Atmos. Chem. Phys., 11, 1155–1165, doi:10.5194/acp-11-1155-2011, 2011.

Eddingsaas, N. C., Loza, C. L., Yee, L. D., Chan, M., Schilling, K. A., Chhabra, P. S., Seinfeld, J. H., and Wennberg, P. O.: α-pinene photooxidation under controlled chemical conditions – Part 2: SOA yield and composition in low- and high-NO_x environments, Atmos. Chem. Phys., 12, 7413–7427, doi:10.5194/acp-12-7413-2012, 2012.

Farina, S. C., Adams, P. J., and Pandis, S. N.: Modeling global secondary organic aerosol formation and processing with the volatility basis set: implications for anthropogenic secondary organic aerosol, J. Geophys. Res.-Atmos., 115, D09202, doi:10.1029/2009JD013046, 2010.

Fisseha, R., Dommen, J., Sax, M., Paulsen, D., Kalberer, M., Maurer, R., Höfler, F., Weingartner, E., and Baltensperger, U.: Identification of organic acids in secondary organic aerosol and the corresponding gas phase from chamber experiments, Anal. Chem., 76, 6535–6540, doi:10.1021/ac048975f, 2004.

Forstner, H. J. L., Flagan, R. C., and Seinfeld, J. H.: Secondary organic aerosol from the photooxidation of aromatic hydrocarbons: molecular composition, Environ. Sci. Technol., 31, 1345–1358, doi:10.1021/es9605376, 1997.

Hallquist, M., Wenger, J. C., Baltensperger, U., Rudich, Y., Simpson, D., Claeys, M., Dommen, J., Donahue, N. M., George, C., Goldstein, A. H., Hamilton, J. F., Herrmann, H., Hoffmann, T., Iinuma, Y., Jang, M., Jenkin, M. E., Jimenez, J. L., Kiendler-Scharr, A., Maenhaut, W., McFiggans, G., Mentel, Th. F., Monod, A., Prévôt, A. S. H., Seinfeld, J. H., Surratt, J. D., Szmigielski, R., and Wildt, J.: The formation, properties and impact of secondary organic aerosol: current and emerging issues, Atmos. Chem. Phys., 9, 5155–5236, doi:10.5194/acp-9-5155-2009, 2009.

ACPD

doi:10.5194/acp-2015-871

Hamilton, J. F., Webb, P. J., Lewis, A. C., and Reviejo, M. M.: Quantifying small molecules in secondary organic aerosol formed during the photo-oxidation of toluene with hydroxyl radicals, Atmos. Environ., 39, 7263–7275, doi:10.1016/j.atmosenv.2005.09.006, 2005.

Heald, C. L., Goldstein, A. H., Allan, J. D., Aiken, A. C., Apel, E., Atlas, E. L., Baker, A. K., Bates, T. S., Beyersdorf, A. J., Blake, D. R., Campos, T., Coe, H., Crounse, J. D., DeCarlo, P. F., de Gouw, J. A., Dunlea, E. J., Flocke, F. M., Fried, A., Goldan, P., Griffin, R. J., Herndon, S. C., Holloway, J. S., Holzinger, R., Jimenez, J. L., Junkermann, W., Kuster, W. C., Lewis, A. C., Meinardi, S., Millet, D. B., Onasch, T., Polidori, A., Quinn, P. K., Riemer, D. D., Roberts, J. M., Salcedo, D., Sive, B., Swanson, A. L., Talbot, R., Warneke, C., Weber, R. J., Weibring, P., Wennberg, P. O., Worsnop, D. R., Wittig, A. E., Zhang, R., Zheng, J., and Zheng, W.: Total observed organic carbon (TOOC) in the atmosphere: a synthesis of North American observations, Atmos. Chem. Phys., 8, 2007–2025, doi:10.5194/acp-8-2007-2008, 2008.

Heald, C. L., Kroll, J. H., Jimenez, J. L., Docherty, K. S., DeCarlo, P. F., Aiken, A. C., Chen, Q., Martin, S. T., Farmer, D. K., and Artaxo, P.: A simplified description of the evolution of organic aerosol composition in the atmosphere, Geophys. Res. Lett., 37, L08803, doi:10.1029/2010GL042737, 2010.

Henze, D. K., Seinfeld, J. H., Ng, N. L., Kroll, J. H., Fu, T.-M., Jacob, D. J., and Heald, C. L.: Global modeling of secondary organic aerosol formation from aromatic hydrocarbons: high- vs. low-yield pathways, Atmos. Chem. Phys., 8, 2405–2420, doi:10.5194/acp-8-2405-2008, 2008.

Hu, L., Millet, D. B., Baasandorj, M., Griffis, T. J., Travis, K. R., Tessum, C. W., Marshall, J. D., Reinhart, W. F., Mikoviny, T., Müller, M., Wisthaler, A., Graus, M., Warneke, C., and de Gouw, J.: Emissions of C_6–C_8 aromatic compounds in the United States: constraints from tall tower and aircraft measurements, J. Geophys. Res.-Atmos., 120, 826–842, doi:10.1002/2014JD022627, 2015.

Huang, M., Zhang, W., Hao, L., Wang, Z., Zhao, W., Gu, X., Guo, X., Liu, X., Long, B., and Fang, L.: Laser desorption/ionization mass spectrometric study of secondary organic aerosol formed from the photooxidation of aromatics, J. Atmos. Chem., 58, 237–252, doi:10.1007/s10874-007-9090-x, 2007.

Huang, M., Wang, Z., Hao, L., and Zhang, W.: Theoretical investigation on the mechanism and kinetics of OH radical with ethylbenzene: Int. J. Quantum. Chem., 111, 3125–3134, doi:10.1002/qua.22751, 2011.

ACPD
doi:10.5194/acp-2015-871

IPCC: Intergovernmental Panel on Climate Change: Climate Change 2007: The Physical Science Basis, Cambridge University Press, UK, 6, 07, 2007.

Izumi, K. and Fukuyama, T.: Photochemical aerosol formation from aromatic hydrocarbons in the presence of NO_x, Atmos. Environ., 24, 1433–1441, doi:10.1016/0960-1686(90)90052-O, 1990.

Kaiser, E. W., Siegl, W. O., Cotton, D. F., and Anderson, R. W.: Effect of fuel structure on emissions from a spark-ignited engine. 2. Naphthene and aromatic fuels, Environ. Sci. Technol., 26, 1581–1586, doi:10.1021/es00032a014, 1992.

Kalberer, M., Paulsen, D., Sax, M., Steinbacher, M., Dommen, J., Prevot, A. S. H., Fisseha, R., Weingartner, E., Frankevich, V., and Zenobi, R.: Identification of polymers as major components of atmospheric organic aerosols, Science, 303, 1659–1662, doi:10.1126/science.1092185, 2004.

Kanakidou, M., Seinfeld, J. H., Pandis, S. N., Barnes, I., Dentener, F. J., Facchini, M. C., Van Dingenen, R., Ervens, B., Nenes, A., Nielsen, C. J., Swietlicki, E., Putaud, J. P., Balkanski, Y., Fuzzi, S., Horth, J., Moortgat, G. K., Winterhalter, R., Myhre, C. E. L., Tsigaridis, K., Vignati, E., Stephanou, E. G., and Wilson, J.: Organic aerosol and global climate modelling: a review, Atmos. Chem. Phys., 5, 1053–1123, doi:10.5194/acp-5-1053-2005, 2005.

Kansal, A.: Sources and reactivity of NMHCs and VOCs in the atmosphere: a review, J. Hazard. Mater., 166, 17–26, doi:10.1016/j.jhazmat.2008.11.048, 2009.

Katrib, Y., Martin, S. T., Rudich, Y., Davidovits, P., Jayne, J. T., and Worsnop, D. R.: Density changes of aerosol particles as a result of chemical reaction, Atmos. Chem. Phys., 5, 275–291, doi:10.5194/acp-5-275-2005, 2005.

Krewski, D., Burnett, R., Goldberg, M., Hoover, B. K., Siemiatycki, J., Jerrett, M., Abrahamowicz, M., and White, W.: Overview of the reanalysis of the Harvard six cities study and American Cancer Society study of particulate air pollution and mortality, Toxicol. Env. Heal. A, 66, 1507–1552, doi:10.1080/15287390306424, 2003.

Kuwata, M., Zorn, S. R., and Martin, S. T.: Using elemental ratios to predict the density of organic material composed of carbon, hydrogen, and oxygen, Environ. Sci. Technol., 46, 787–794, doi:10.1021/es202525q, 2011.

Lambe, A. T., Onasch, T. B., Croasdale, D. R., Wright, J. P., Martin, A. T., Franklin, J. P., Massoli, P., Kroll, J. H., Canagaratna, M. R., Brune, W. H., Worsnop, D. R., and Davidovits, P.: Transitions from functionalization to fragmentation reactions of laboratory secondary organic

ACPD
doi:10.5194/acp-2015-871

aerosol (SOA) generated from the OH oxidation of alkane precursors, Environ. Sci. Technol., 46, 5430–5437, doi:10.1021/es300274t, 2012.

Lambe, A. T., Chhabra, P. S., Onasch, T. B., Brune, W. H., Hunter, J. F., Kroll, J. H., Cummings, M. J., Brogan, J. F., Parmar, Y., Worsnop, D. R., Kolb, C. E., and Davidovits, P.: Effect of oxidant concentration, exposure time, and seed particles on secondary organic aerosol chemical composition and yield, Atmos. Chem. Phys., 15, 3063–3075, doi:10.5194/acp-15-3063-2015, 2015.

Li, L., Tang, P., Nakao, S., Chen, C.-L., and Cocker III, D. R.: Role of methyl group number on SOA formation from aromatic hydrocarbons photooxidation under low NO_x conditions, Atmos. Chem. Phys. Discuss., 15, 31153–31196, doi:10.5194/acpd-15-31153-2015, 2015a.

Li, L., Tang, P., and Cocker III, D. R.: Instantaneous nitric oxide effect on secondary organic aerosol formation from *m*-xylene photooxidation, Atmos. Environ, 119, 144–155, doi:10.1016/j.atmosenv.2015.08.010, 2015b.

Lim, Y. B. and Ziemann, P. J.: Effects of molecular structure on aerosol yields from OH radical-initiated reactions of linear, branched, and cyclic alkanes in the presence of NO_x, Environ. Sci. Technol., 43, 2328–2334, doi:10.1021/es803389s, 2009.

Lough, G. C., Schauer, J. J., Lonneman, W. A., and Allen, M. K.: Summer and winter non-methane hydrocarbon emissions from on-road motor vehicles in the Midwestern United States, J. Air. Waste. Manage., 55, 629–646, doi:10.1080/10473289.2005.10464649, 2005

Loza, C. L., Chhabra, P. S., Yee, L. D., Craven, J. S., Flagan, R. C., and Seinfeld, J. H.: Chemical aging of *m*-xylene secondary organic aerosol: laboratory chamber study, Atmos. Chem. Phys., 12, 151–167, doi:10.5194/acp-12-151-2012, 2012.

Loza, C. L., Craven, J. S., Yee, L. D., Coggon, M. M., Schwantes, R. H., Shiraiwa, M., Zhang, X., Schilling, K. A., Ng, N. L., Canagaratna, M. R., Ziemann, P. J., Flagan, R. C., and Seinfeld, J. H.: Secondary organic aerosol yields of 12-carbon alkanes, Atmos. Chem. Phys., 14, 1423–1439, doi:10.5194/acp-14-1423-2014, 2014.

Malloy, Q. G., Nakao, S., Qi, L., Austin, R., Stothers, C., Hagino, H., and Cocker III, D. R.: Real-time aerosol density determination utilizing a modified scanning mobility particle sizer – aerosol particle mass analyzer system, Aerosol. Sci. Tech., 43, 673–678, doi:10.1080/02786820902832960, 2009.

Matsui, H., Koike, M., Takegawa, N., Kondo, Y., Griffin, R., Miyazaki, Y., Yokouchi, Y., and Ohara, T.: Secondary organic aerosol formation in urban air: temporal variations and pos-

ACPD
doi:10.5194/acp-2015-871

sible contributions from unidentified hydrocarbons, J. Geophys. Res.-Atmos, 114, D04201, doi:10.1029/2008JD010164, 2009.
Millet, D. B., Donahue, N. M., Pandis, S. N., Polidori, A., Stanier, C. O., Turpin, B. J., and Goldstein, A. H.: Atmospheric volatile organic compound measurements during the Pittsburgh Air Quality Study: results, interpretation, and quantification of primary and secondary contributions, J. Geophys. Res.-Atmos, 110, D07S07, doi:10.1029/2004JD004601, 2005
Miracolo, M. A., Drozd, G. T., Jathar, S. H., Presto, A. A., Lipsky, E. M., Corporan, E., and Robinson, A. L.: Fuel composition and secondary organic aerosol formation: gas-turbine exhaust and alternative aviation fuels, Environ. Sci. Technol., 46, 8493–8501, doi:10.1021/es300350c, 2012.
Monod, A., Sive, B. C., Avino, P., Chen, T., Blake, D. R., and Rowland, F. S.: Monoaromatic compounds in ambient air of various cities: a focus on correlations between the xylenes and ethylbenzene, Atmos. Environ., 35, 135–149, doi:10.1016/S1352-2310(00)00274-0, 2001.
Na, K., Moon, K.-C., and Kim, Y. P.: Source contribution to aromatic VOC concentration and ozone formation potential in the atmosphere of Seoul, Atmos. Environ., 39, 5517–5524, doi:10.1016/j.atmosenv.2005.06.005, 2005.
Nakao, S., Clark, C., Tang, P., Sato, K., and Cocker III, D.: Secondary organic aerosol formation from phenolic compounds in the absence of NO_x, Atmos. Chem. Phys., 11, 10649–10660, doi:10.5194/acp-11-10649-2011, 2011.
Nakao, S., Liu, Y., Tang, P., Chen, C.-L., Zhang, J., and Cocker III, D. R.: Chamber studies of SOA formation from aromatic hydrocarbons: observation of limited glyoxal uptake, Atmos. Chem. Phys., 12, 3927–3937, doi:10.5194/acp-12-3927-2012, 2012.
Ng, N. L., Kroll, J. H., Chan, A. W. H., Chhabra, P. S., Flagan, R. C., and Seinfeld, J. H.: Secondary organic aerosol formation from *m*-xylene, toluene, and benzene, Atmos. Chem. Phys., 7, 3909–3922, doi:10.5194/acp-7-3909-2007, 2007.
Ng, N. L., Canagaratna, M. R., Zhang, Q., Jimenez, J. L., Tian, J., Ulbrich, I. M., Kroll, J. H., Docherty, K. S., Chhabra, P. S., Bahreini, R., Murphy, S. M., Seinfeld, J. H., Hildebrandt, L., Donahue, N. M., DeCarlo, P. F., Lanz, V. A., Prévôt, A. S. H., Dinar, E., Rudich, Y., and Worsnop, D. R.: Organic aerosol components observed in Northern Hemispheric datasets from Aerosol Mass Spectrometry, Atmos. Chem. Phys., 10, 4625–4641, doi:10.5194/acp-10-4625-2010, 2010.

ACPD
doi:10.5194/acp-2015-871

Ng, N. L., Canagaratna, M. R., Jimenez, J. L., Chhabra, P. S., Seinfeld, J. H., and Worsnop, D. R.: Changes in organic aerosol composition with aging inferred from aerosol mass spectra, Atmos. Chem. Phys., 11, 6465–6474, doi:10.5194/acp-11-6465-2011, 2011.

Odum, J. R., Hoffmann, T., Bowman, F., Collins, D., Flagan, R. C., and Seinfeld, J. H.: Gas/particle partitioning and secondary organic aerosol yields, Environ. Sci. Technol., 30, 2580–2585, doi:10.1021/es950943+, 1996.

Odum, J. R., Jungkamp, T., Griffin, R., Flagan, R. C., and Seinfeld, J. H.: The atmospheric aerosol-forming potential of whole gasoline vapor, Science, 276, 96–99, doi:10.1126/science.276.5309.96, 1997a.

Odum, J. R., Jungkamp, T., Griffin, R. J., Forstner, H., Flagan, R. C., and Seinfeld, J. H.: Aromatics, reformulated gasoline, and atmospheric organic aerosol formation, Environ. Sci. Technol., 31, 1890–1897, doi:10.1021/es960535l, 1997b.

Pöschl, U.: Atmospheric aerosols: composition, transformation, climate and health effects, Angew. Chem. Int. Edit., 44, 7520–7540, doi:10.1002/anie.200501122, 2005.

Pang, Y., Turpin, B., and Gundel, L.: On the importance of organic oxygen for understanding organic aerosol particles, Aerosol. Sci. Tech., 40, 128–133, doi:10.1080/02786820500423790, 2006.

Pfaffenberger, L., Barmet, P., Slowik, J. G., Praplan, A. P., Dommen, J., Prévôt, A. S. H., and Baltensperger, U.: The link between organic aerosol mass loading and degree of oxygenation: an α-pinene photooxidation study, Atmos. Chem. Phys., 13, 6493–6506, doi:10.5194/acp-13-6493-2013, 2013.

Qi, L., Nakao, S., Malloy, Q., Warren, B., and Cocker III, D. R.: Can secondary organic aerosol formed in an atmospheric simulation chamber continuously age?, Atmos. Environ., 44, 2990–2996, doi:10.1016/j.atmosenv.2010.05.020, 2010a.

Qi, L., Nakao, S., Tang, P., and Cocker III, D. R.: Temperature effect on physical and chemical properties of secondary organic aerosol from *m*-xylene photooxidation, Atmos. Chem. Phys., 10, 3847–3854, doi:10.5194/acp-10-3847-2010, 2010b.

Rader, D. J. and McMurry, P. H.: Application of the tandem differential mobility analyzer to studies of droplet growth or evaporation, J. Aerosol. Sci., 17, 771–787, doi:10.1016/0021-8502(86)90031-5, 1986.

Rubin, J. I., Kean, A. J., Harley, R. A., Millet, D. B., and Goldstein, A. H.: Temperature dependence of volatile organic compound evaporative emissions from motor vehicles, J. Geophys. Res.-Atmos., 111, D03305, doi:10.1029/2005JD006458, 2006.

ACPD
doi:10.5194/acp-2015-871

Salo, K., Hallquist, M., Jonsson, Å. M., Saathoff, H., Naumann, K.-H., Spindler, C., Tillmann, R., Fuchs, H., Bohn, B., Rubach, F., Mentel, Th. F., Müller, L., Reinnig, M., Hoffmann, T., and Donahue, N. M.: Volatility of secondary organic aerosol during OH radical induced ageing, Atmos. Chem. Phys., 11, 11055–11067, doi:10.5194/acp-11-11055-2011, 2011.

Sato, K., Hatakeyama, S., and Imamura, T.: Secondary organic aerosol formation during the photooxidation of toluene: NO_x dependence of chemical composition, J. Phys. Chem. A, 111, 9796–9808, doi:10.1021/jp071419f, 2007.

Sato, K., Takami, A., Isozaki, T., Hikida, T., Shimono, A., and Imamura, T.: Mass spectrometric study of secondary organic aerosol formed from the photo-oxidation of aromatic hydrocarbons, Atmos. Environ., 44, 1080–1087, doi:10.1016/j.atmosenv.2009.12.013, 2010.

Sato, K., Takami, A., Kato, Y., Seta, T., Fujitani, Y., Hikida, T., Shimono, A., and Imamura, T.: AMS and LC/MS analyses of SOA from the photooxidation of benzene and 1,3,5-trimethylbenzene in the presence of NO_x: effects of chemical structure on SOA aging, Atmos. Chem. Phys., 12, 4667–4682, doi:10.5194/acp-12-4667-2012, 2012.

Seinfeld, J. and Pandis, S.: Atmospheric Chemistry Physics: From Air Pollution to Climate Change, John Wiley & Sons Publications, Hoboken, New Jersey, US, 2006.

Shilling, J. E., Chen, Q., King, S. M., Rosenoern, T., Kroll, J. H., Worsnop, D. R., DeCarlo, P. F., Aiken, A. C., Sueper, D., Jimenez, J. L., and Martin, S. T.: Loading-dependent elemental composition of α-pinene SOA particles, Atmos. Chem. Phys., 9, 771–782, doi:10.5194/acp-9-771-2009, 2009.

Singh, H. B., Salas, L. J., Cantrell, B. K., and Redmond, R. M.: Distribution of aromatic hydrocarbons in the ambient air, Atmos. Environ., 19, 1911–1919, doi:10.1016/0004-6981(85)90017-4, 1985.

Song, C., Na, K., and Cocker III, D. R.: Impact of the hydrocarbon to NO_x ratio on secondary organic aerosol formation, Environ. Sci. Technol., 39, 3143–3149, doi:10.1021/es0493244, 2005.

Song, C., Na, K., Warren, B., Malloy, Q., and Cocker III, D. R.: Secondary organic aerosol formation from the photooxidation of *p*-and *o*-xylene. Environ. Sci. Technol., 41, 7403–7408, doi:10.1021/es0621041, 2007.

Tkacik, D. S., Presto, A. A., Donahue, N. M., and Robinson, A. L.: Secondary organic aerosol formation from intermediate-volatility organic compounds: cyclic, linear, and branched alkanes, Environ. Sci. Technol., 46, 8773–8781, doi:10.1021/es301112c, 2012.

ACPD
doi:10.5194/acp-2015-871

Tritscher, T., Dommen, J., DeCarlo, P. F., Gysel, M., Barmet, P. B., Praplan, A. P., Weingartner, E., Prévôt, A. S. H., Riipinen, I., Donahue, N. M., and Baltensperger, U.: Volatility and hygroscopicity of aging secondary organic aerosol in a smog chamber, Atmos. Chem. Phys., 11, 11477–11496, doi:10.5194/acp-11-11477-2011, 2011.

Yee, L. D., Kautzman, K. E., Loza, C. L., Schilling, K. A., Coggon, M. M., Chhabra, P. S., Chan, M. N., Chan, A. W. H., Hersey, S. P., Crounse, J. D., Wennberg, P. O., Flagan, R. C., and Seinfeld, J. H.: Secondary organic aerosol formation from biomass burning intermediates: phenol and methoxyphenols, Atmos. Chem. Phys., 13, 8019–8043, doi:10.5194/acp-13-8019-2013, 2013.

Yu, L., Smith, J., Laskin, A., Anastasio, C., Laskin, J., and Zhang, Q.: Chemical characterization of SOA formed from aqueous-phase reactions of phenols with the triplet excited state of carbonyl and hydroxyl radical, Atmos. Chem. Phys., 14, 13801–13816, doi:10.5194/acp-14-13801-2014, 2014.

Zhang, Q., Alfarra, M. R., Worsnop, D. R., Allan, J. D., Coe, H., Canagaratna, M. R., and Jimenez, J. L.: Deconvolution and quantification of hydrocarbon-like and oxygenated organic aerosols based on aerosol mass spectrometry, Environ. Sci. Technol., 39, 4938–4952, doi:10.1021/es048568l, 2005.

Zhang, Y., Wang, X., Barletta, B., Simpson, I. J., Blake, D. R., Fu, X., Zhang, Z., He, Q., Liu, T., Zhao, X., and Ding, X.: Source attributions of hazardous aromatic hydrocarbons in urban, suburban and rural areas in the Pearl River Delta (PRD) region, J. Hazard. Mater., 250, 403–411, doi:10.1016/j.jhazmat.2013.02.023, 2013.

Ziemann, P.: Effects of molecular structure on the chemistry of aerosol formation from the OH-radical-initiated oxidation of alkanes and alkenes, Int. Rev. Phys. Chem., 30, 161–195, doi:10.1080/0144235X.2010.550728, 2011.

Ziemann, P. J. and Atkinson, R.: Kinetics, products, and mechanisms of secondary organic aerosol formation, Chem. Soc. Rev., 41, 6582–6605, doi:10.1039/c2cs35122f, 2012.

ACPD

doi:10.5194/acp-2015-871

Table 1. Experiment conditions.

Precursor	ID	HC/NO[a]	NO[b]	HC[b]	ΔHC[c]	Mo[c]	Yield
Ethylbenzene	1142A	17.0	47.4	101	331	22.0	0.066
	1142B	12.0	66.6	99.9	341	4.40	0.013
	1146A	35.6	22.2	99.0	257	36.0	0.140
	1146B	23.0	34.8	100	331	23.6	0.071
	1147B	74.9	36.5	342	626	88.1	0.141
	2084A	81.1	23.9	242	374	54.0	0.145
	2084B	93.8	20.3	238	266	44.3	0.167
Propylbenzene	1245A	41.0	22.1	101	231	11.8	0.051
	1246A	26.8	68.5	204	421	22.9	0.054
Isopropylbenzene	1247A	40.3	22.4	100	301	33.2	0.110
	1247B	18.6	48.1	99.3	300	16.6	0.055
	1253A	31.9	56.4	200.	538	53.1	0.099
	1253B[d]	17.6	100	196	526	16.5	0.031
o-Xylene	1315A	13.2	49.8	82.2	324	26.3	0.081
	1315B	28.8	22.2	80.0	27	25.4	0.091
	1320A	12.8	50.0	80.0	335	18.4	0.055
	1321A	31.0	20.5	79.2	263	16.2	0.061
	1321B	61.3	10.4	80.0	226	9.80	0.044
p-Xylene	1308A	15.5	55.6	78.4	279	6.80	0.024
	1308B	171	22.9	78.8	274	11.3	0.041
m-Ethyltoluene	1151A	17.9	62.5	84.8	409	8.30	0.020
	1151B	31.0	32.3	86.4	415	28.7	0.069
	1199A	8.8	45.4	100.2	447	72.0	0.161
	1222B	41.7	69.4	100.0	484	70.9	0.146
	1226B	11.3	137.6	201.1	895	138	0.154
	1232A	27.5	122.0	200.0	901	150	0.167
	1232B	33.1	67.5	194.8	751	117	0.155
	1421A	41.0	22.1	97.9	409	46.2	0.112
	1421B	18.0	44.9	98.7	477	54.6	0.114

ACPD
doi:10.5194/acp-2015-871

Table 1. Continued.

Precursor	ID	HC/NO[a]	NO[b]	HC[b]	ΔHC[c]	Mo[c]	Yield
o-Ethyltoluene	1179A	16.3	52.9	91.7	399	86.5	0.216
	1179B	15.8	52.9	93.0	415	75.3	0.181
	1202A	18.5	60.3	99.7	422	69.9	0.166
	1215A	29.2	107.9	180.3	637	1501	0.237
	1413A	12.2	21.3	100.4	371	64.5	0.174
	1413B	24.1	45.8	98.4	455	64.4	0.141
p-Ethyltoluene	1194A	19.9	90.7	196	741	90.4	0.122
	1194B	13.0	88.4	200	761	73.0	0.096
	1197A	13.1	56.4	192	653	66.4	0.102
	1197B	14.8	98.5	192	710	58.4	0.082
	1214B	26.0	53.4	102	418	29.1	0.069
	1601A	39.9	31.2	109	452	17.6	0.039
1,2,3-Trimethylbenzene	1158A	19.8	10.3	79.9	296	22.2	0.075
	1158B	15.6	22.4	79.9	379	32.3	0.085
	1162A	15.8	33.4	80.1	391	46.5	0.119
	1162B	14.9	40.0	80.4	399	46.6	0.117
1,3,5-Trimethylbenzene	1153A	65.2	11.0	79.5	309	12.4	0.040
	1153B	35.3	20.4	80	381	19.6	0.051
	1156A	22.3	32.3	80.2	379	24.8	0.065
	1156B	15.5	46.1	79.6	390	19.0	0.049
	1329B	11.1	64.8	80.0	296	3.00	0.007

Note: [a] unit of HC/NO are ppbC : ppb; [b] unit of NO and HC are ppb; [c] unit of ΔHC and M_0 are $\mu g\,m^{-3}$, M_0 is a wall loss and density corrected particle mass concentration; [d] not used in curve fitting.

ACPD
doi:10.5194/acp-2015-871

Table 2. Two product yield curve fitting parameters for one, two (ortha, meta and para) and three alkyl substitutes.

Yield Curve	α_1	$K_{om,1}$ ($m^3\ \mu g^{-1}$)	α_2	$K_{om,2}$ ($m^3\ \mu g^{-1}$)
One Substitutes	0.144	0.039	0.137	0.005
Two Substitutes-ortho	0.158	0.249	0.024	0.005
Two Substitutes-meta	0.156	0.040	0.080	0.005
Two Substitutes-para	0.154	0.025	0.036	0.005
Three Substitutes	0.180	0.025	0.052	0.005

ACPD
doi:10.5194/acp-2015-871

Table 3. Correlation among SOA density, volatility (VFR) and SOA chemical composition.

	f_{44}	f_{57}	f_{71}	O/C	H/C	OS_c	k_{OH}
Density	0.324	−0.056	−0.38	0.551	−0.301	0.540	−0.249
p value[b]	0.304	0.862	0.223	0.063	0.341	0.070	0.435
VFR_{end}[a]	0.537	0.56	0.399	0.471	−0.586	0.593	−0.937
p value[b]	0.089	0.073	0.224	0.144	0.058	0.055	0

Note: [a] VFR_{end} volume fraction remaining at the end of photooxidation; [b] p values range from 0 to 1, 0-reject null hypothesis and 1 accept null hypothesis. Alpha (α) level used is 0.05. If the p value of a test statistic is less than alpha, the null hypothesis is rejected.

ACPD
doi:10.5194/acp-2015-871

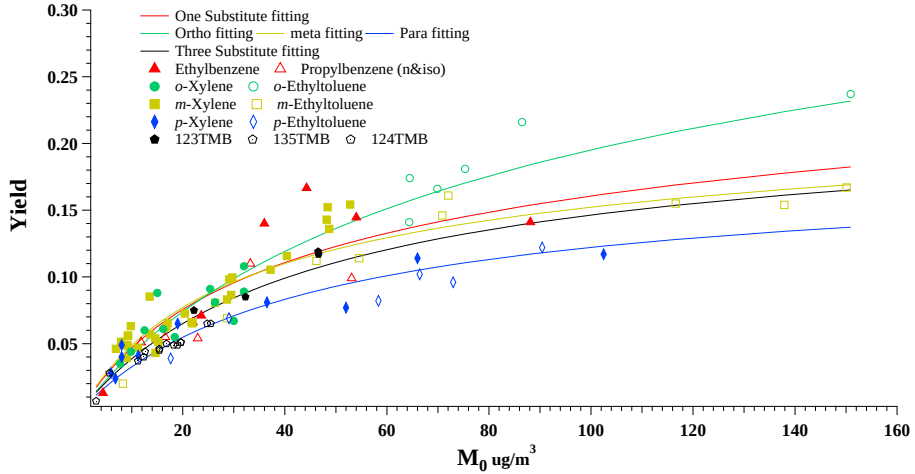

Figure 1. Aromatic SOA yields as a function of M_0. (Note: Song et al., 2005, 2007; Li et al., 2015a data are also included; 123TMB – 1,2,3-Trimethylbenzene; 135TMB – 1,3,5-Trimethylbenzene; 124TMB – 1,2,4-Trimethylbenzene.)

ACPD
doi:10.5194/acp-2015-871

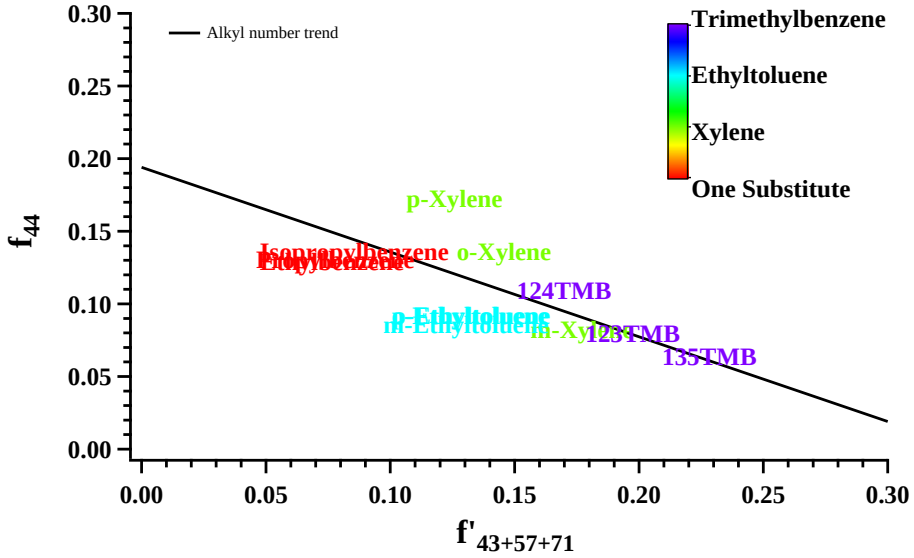

Figure 2. f_{44+} vs. $f'_{43+57+71}$ in SOA formed from different aromatic hydrocarbon photooxidation under low NO_x colored by aromatic isomer type and marked with individual aromatic hydrocarbon species: Ethylbenzene 2084A; Propylbenzene 1245A; Isopropylbenzene 1247A; *m*-Xylene 1191A; *m*-Ethyltoluene 1199A; *o*-Xylene 1320A; *o*-Ethyltoluene 1179A; *p*-Xylene 1308A; *p*-Ethyltoluene 1194A; 1,2,3-Trimethylbenzene (123TMB) 1162A; 1,2,4-Trimethylbenzene (124TMB) 1119A; 1,3,5-Trimethylbenzene (135TMB) 1156A. Alkyl number trend is the linear fitting in (Li et al., 2015a).

ACPD
doi:10.5194/acp-2015-871

Impact of molecular structure on SOA formation

L. Li et al.

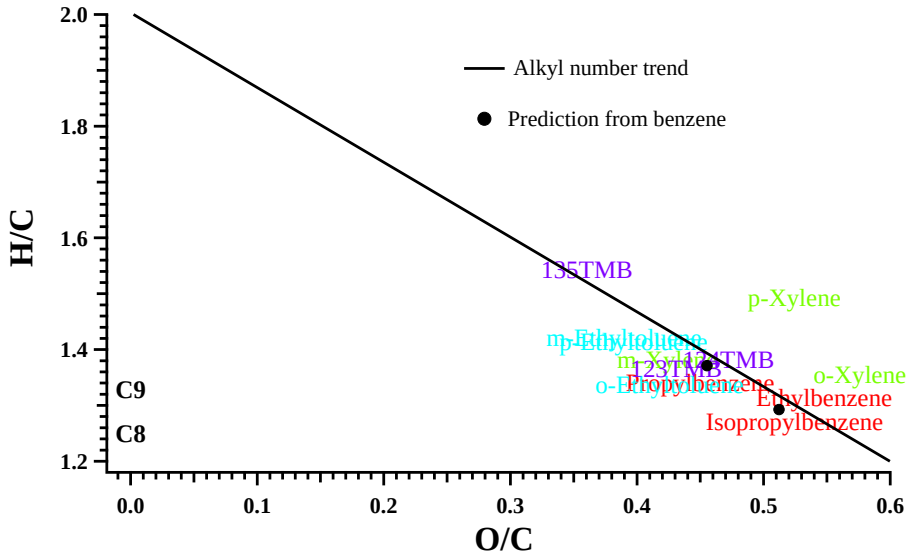

Figure 3. H/C vs. O/C in SOA formed from different aromatic hydrocarbon photooxidation under low NO_x colored by aromatic isomer type and marked with individual aromatic hydrocarbon species (C8 and C9 on the lower left indicate the location of initial aromatic hydrocarbon precursor): Ethylbenzene 2084A; Propylbenzene 1245A; Isopropylbenzene 1247A; *m*-Xylene 1191A; *m*-Ethyltoluene 1199A; *o*-Xylene 1320A; *o*-Ethyltoluene 1179A; *p*-Xylene 1308A; *p*-Ethyltoluene 1194A; 1,2,3-Trimethylbenzene (123TMB) 1162A; 1,2,4-Trimethylbenzene(124TMB) 1119A; 1,3,5-Trimethylbenzene(135TMB) 1156A. Alkyl number trend is the linear fitting in (Li et al., 2015a). Solid black cycles are SOA elemental ratio from C_8 and C_9 aromatic hydrocarbon predicted by SOA elemental ratio formed from benzene.

ACPD
doi:10.5194/acp-2015-871

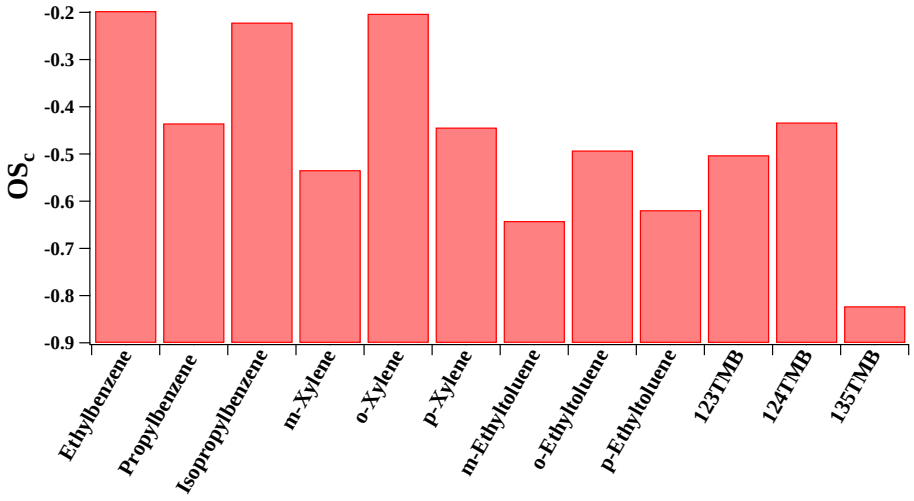

Figure 4. Oxidation state (OS_c) of SOA formed from different aromatic hydrocarbon photooxidation under low NO_x: Ethylbenzene 2084A; Propylbenzene 1245A; Isopropylbenzene 1247A; *m*-Xylene 1191A; *m*-Ethyltoluene 1199A; *o*-Xylene 1320A; *o*-Ethyltoluene 1179A; *p*-Xylene 1308A; *p*-Ethyltoluene 1194A; 1,2,3-Trimethylbenzene (123TMB) 1162A; 1,2,4-Trimethylbenzene(124TMB) 1119A; 1,3,5-Trimethylbenzene(135TMB) 1156A.

ACPD
doi:10.5194/acp-2015-871

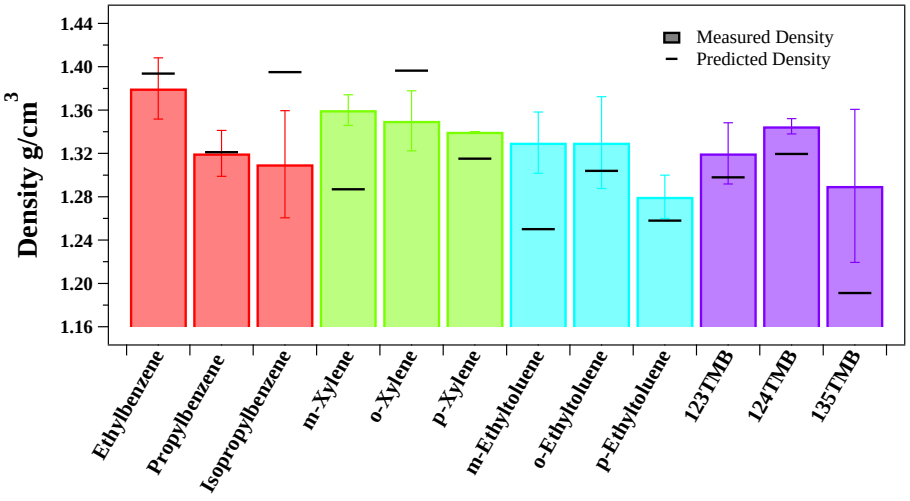

Figure 5. Measured and predicted SOA density from different aromatic hydrocarbon photooxidation under low NO_x (Colored with substitute number and length, one substitute-red, xylenes-green, ethyltoluenes-blue and trimethylbenzene-purple; black line is predicted density according to Kuwata et al., 2011); 123TMB – 1,2,3-Trimethylbenzene; 135TMB – 1,3,5-Trimethylbenzene; 124TMB – 1,2,4-Trimethylbenzene.

ACPD
doi:10.5194/acp-2015-871

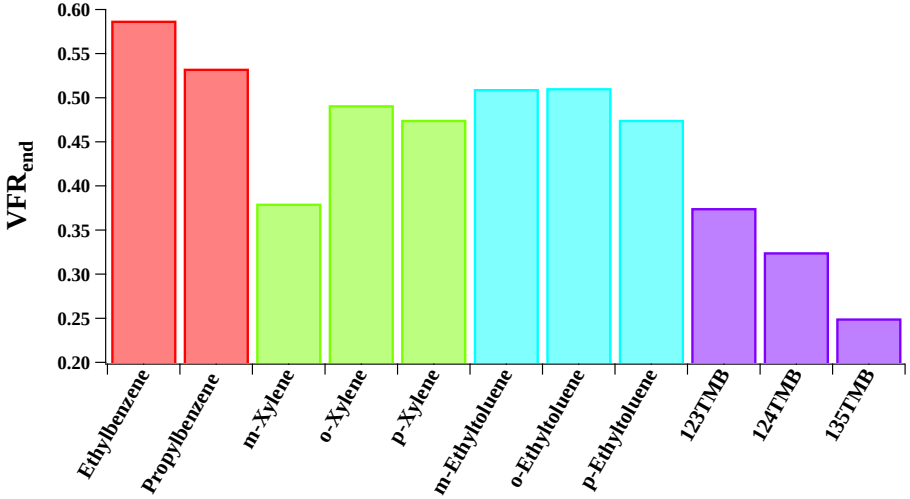

Figure 6. SOA Volume fraction remaining (VFR_{end}) at the end of aromatic hydrocarbon photooxidation under low NO_x (Colored with substitute number and length, one substitute-red, xylenes-green, ethyltoluenes-blue and trimethylbenzene-purple); 123TMB – 1,2,3-Trimethylbenzene; 135TMB – 1,3,5-Trimethylbenzene; 124TMB – 1,2,4-Trimethylbenzene.

ACPD
doi:10.5194/acp-2015-871

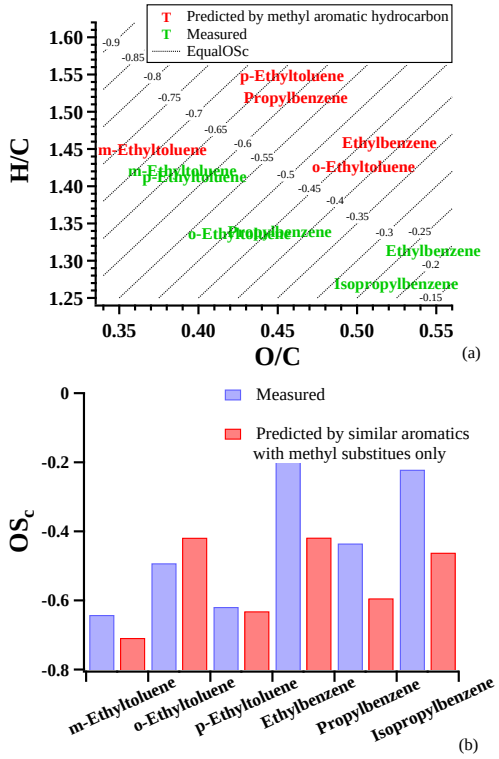

Figure 7. Comparison of measured and predicted elemental ratio **(a)** and oxidation state **(b)** of SOA formed from longer alkyl substitute ($-C_2H_{2n+1}$, $n > 1$). Ethyltoluenes are predicted by corresponding xylenes and one substitute aromatic hydrocarbons are predicted by toluene. *Predicted elemental ratio of isopropylbenzene is same as propylbenzene (not showed in **a**).

ACPD
doi:10.5194/acp-2015-871

Impact of molecular structure on SOA formation

L. Li et al.